Molecular detection of infection homogeneity and impact of miltefosine treatment in a Syrian golden hamster model of Leishmania donovani and L. infantum visceral leishmaniasis

Title

Molecular detection of infection homogeneity and impact of miltefosine treatment in a Syrian Golden hamster model of *Leishmania donovani* and *L. infantum* visceral leishmaniasis

Short title

Detection of tissue-level homogeneity of *Leishmania* infection and impact of miltefosine treatment

Authors and affiliations

Eline Eberhardt[†], Annelies Mondelaers[†], Sarah Hendrickx, Magali Van den Kerkhof, Louis Maes[†], Guy Caljon[†*]

Laboratory of Microbiology, Parasitology and Hygiene (LMPH), University of Antwerp, Wilrijk, Belgium

[†] Equal contribution

*corresponding author: Guy Caljon

Laboratory of Microbiology, Parasitology and Hygiene (LMPH), Room S7.24,

Campus Drie Eiken, Universiteitsplein 1, B-2610 Wilrijk, Belgium

Guy.Caljon@uantwerpen.be

Tel.: 0032(0)32652601

Abstract

Control of visceral leishmaniasis caused by *Leishmania infantum* and *L. donovani* primarily relies on chemotherapy using an increasingly compromised repertoire of antileishmanial compounds. For evaluation of novel drugs, the Syrian golden hamster is considered as a clinically relevant laboratory model. In this study, two molecular parasite detection assays were developed targeting *cathepsin-like cysteine protease B* (*CPB*) DNA and *18S rRNA* to achieve absolute amastigote quantification in the major target organs liver and spleen. Both qPCR techniques showed excellent agreement with a strong correlation to the conventional microscopic reading of Giemsa-stained tissue smears. Using multiple single tissue pieces and all three detection methods, we confirmed homogeneity of infection in liver and spleen and the robustness of extrapolating whole organ burdens from a small single tissue piece. Comparison of pre- and post-treatment burdens in infected hamsters using the three detection methods consistently revealed a stronger parasite reduction in the spleen compared to the liver, indicating an organ-dependent clearance efficacy for miltefosine. In conclusion, this study in the hamster demonstrated high homogeneity of infection in liver and spleen and advocates the use of molecular detection methods for assessment of low (post-treatment) tissue burdens.

Keywords:

Visceral Leishmaniasis, infection homogeneity, miltefosine, microscopy, real-time PCR, liver, spleen

Introduction

Visceral leishmaniasis (VL) is a major neglected disease caused by *Leishmania donovani* and *L. infantum* with 300.000 cases worldwide and more than 20.000 deaths annually (WHO 2015a, b). Control of the disease is primarily based on chemotherapy with pentavalent antimonials, amphotericin B, miltefosine and paromomycin (WHO 2015a). However, treatment failures have become more frequent and parasites may acquire resistance fairly easily (Hendrickx et al. 2014, Hendrickx et al. 2015, Purkait et al. 2012, Sundar 2001), urging for the development of novel antileishmanial compounds and close surveillance of existing therapies. After completion of a treatment regimen, patients are generally followed-up for several months to monitor potential relapses and to determine a definite treatment outcome. The former standard microscopic detection of amastigotes in organ smears combined with parasite isolation as promastigotes is now being replaced by molecular techniques, such as PCR, to detect *Leishmania* infection in blood and tissue samples (Bourgeois et al. 2008, WHO 2010).

Syrian golden hamsters can be considered as the more appropriate laboratory model for *in vivo* drug efficacy studies as they reproduce similar clinico-pathological features as symptomatic VL patients with fatal outcome (Loria-Cervera and Andrade-Narvaez 2014, Requena et al. 2000). This contrasts with the more frequently used BALB/c mice that are able to control the infection after an initial acute phase, resulting in a subclinical disease state (Mukherjee et al. 2003, Murray 2001). Parasite burdens in liver and spleen serve as markers for disease status in both animal models and are most commonly determined by microscopy or quantitative PCR (qPCR). Microscopic counting of organ imprints is still considered the gold standard technique for *Leishmania* quantification in animal models (Bretagne et al. 2001, van den Bogaart et al. 2014). However, limited sensitivity (less than 200 parasites/mg tissue cannot be detected when assessing 1000 cell nuclei) makes this technique less suited for evaluating low parasite burdens present after treatment or in asymptomatic infections (Bretagne et al. 2001, Stauber 1958). Hence, qPCR has been explored as a valid alternative because of its improved accuracy and reproducibility (Bretagne et al. 2001, Mary et al. 2004, Tellevik et al. 2014). Another quantitative method, *e.g.* the limiting dilution technique, was not considered in this study as it is time consuming

and less suited for absolute parasite quantification (Srivastava et al. 2013). Furthermore, this technique does not perform well on liver samples since enzymes and bile salts affect parasite viability after isolation (Personal observation).

In this study, infected (high burden) and miltefosine-treated (low burden) Syrian golden hamsters served as a model for the assessment of two novel qPCR techniques targeting *cathepsin-like cysteine Protease B* (*CPB*) DNA and *18S rRNA*, comparing and correlating these quantifications for the first time with the standard microscopic counting method upon Giemsa-staining. Particular attention was given to the extrapolation of parasite burdens in small tissue subsamples for the quantification of whole organ burdens. As both microscopy and qPCR use very small pieces of the organ obtained at a random location, homogeneous distribution of infection over the entire organ is generally assumed, but surprisingly still fairly poorly documented. To the best of our knowledge, no research regarding this topic has been performed in the hamster model. The present study therefore investigated the homogeneity of splenic and hepatic parasite distribution by evaluating livers and spleens of hamsters with high and low *L. infantum* or *L. donovani* parasitism.

In summary, the present work demonstrates the high reproducibility of the VL model in Syrian golden hamsters and a very good agreement of the molecular parasite detection techniques targeting DNA or RNA with the standard microscopic quantification. Homogeneity of infection was demonstrated in both target organs, irrespective of the *Leishmania* species and whether or not treatment was applied, validating quantifications based on a single tissue subsample. Furthermore, this approach was able to detect a differential impact of miltefosine treatment on the two main target organs.

Material and methods

Ethics statement

The use of laboratory rodents was carried out in strict accordance to all mandatory guidelines (European Union directive 2010/63/EU on the protection of animals used for scientific purposes and

the Declaration of Helsinki) and was approved by the ethical committee of the University of Antwerp (UA-ECD 2011-74).

Animals

Female Syrian golden hamsters (body weight 80 to 100 g) were purchased from Janvier (Genest-Saint-Isle, France) and kept in quarantine for at least 5 days before infection. Food for laboratory rodents (Carfil, Arendonk, Belgium) and drinking water were available *ad libitum*.

***Leishmania* parasites, infection and treatment**

Leishmania infantum (MHOM/MA[BE]/67/ITMAP263) and *L. donovani* (MHOM/ET/67/L82) were maintained *in vivo* in Syrian golden hamsters. *Ex vivo* amastigotes were isolated from the spleens of heavily infected donor hamsters and quantified by determining the Stauber index (Stauber 1958). Hamsters were infected intracardially (6 with *L. infantum* and 4 with *L. donovani*) under isoflurane inhalation anaesthesia with an infection inoculum containing 2 x 10^7 amastigotes in 100 µL phosphate buffered saline (PBS). At 21 days post-infection (dpi), half of the animals was treated orally with 40 mg/kg miltefosine (Sigma-Aldrich, Belgium) in PBS for five consecutive days. The animals were closely monitored by evaluating their general condition and body weight twice weekly. Ten days after the last treatment dose, animals were euthanized with a CO_2 overdose and spleens and livers were collected. For assessing the homogeneity of infection, five small pieces were cut at different locations of each organ. Of each tissue piece, an imprint for Giemsa staining was made after which samples were processed for DNA and RNA isolation (<20 mg liver, <10 mg spleen).

Parasite quantification by microscopic evaluation of Giemsa-stained organ imprints

Tissue imprints were fixed with methanol for 2 minutes and stained with a 1:5 Giemsa-dilution (Sigma-Aldrich, Belgium) in MilliQ water. Intracellular amastigote burdens were assessed microscopically by calculating the Stauber index (Stauber 1958):

$$\frac{\#\text{amastigotes counted}}{500\ \text{nuclei}} \text{ x weight organ (mg) x } 200.000$$

The resulting value was divided by the organ weight (g) to obtain the number of amastigotes per gram tissue, which could then be compared to the results obtained by the DNA and RNA qPCR.

RNA extraction and parasite quantification by RNA qPCR

Isolated tissue pieces for the assessment of homogeneity of infection were immediately preserved in RNA later (Qiagen) and stored at -20°C. For RNA extraction, tissues were transferred to RLT buffer supplemented with β-mercaptoethanol and homogenized with a Tissue Ruptor (Qiagen). RNA was purified from liver and spleen homogenates using RNeasy Mini Kit (Qiagen) following the manufacturer's instructions. The resulting RNA was treated with RQ1 RNase-Free DNase (Promega, the Netherlands) to remove genomic DNA from the sample. The RNA concentration and purity was measured with a NanoDrop2000c spectrophotometer (Thermo Scientific). cDNA was synthesized using Accuscript High Fidelity 1st Strand cDNA Synthesis Kit (Agilent Technologies, Belgium). Parasite burdens were quantified using a Taqman qPCR against *18S rRNA*, a highly repetitive gene which is conserved among different *Leishmania* species and has been frequently used (van der Meide et al. 2008, van Eys et al. 1992). Primers and a probe ('*18S rRNA*') were designed to amplify a 121 bp region in the *18S rRNA* gene by using online software (http://www.ncbi.nlm.nih.gov/tools/primer-blast/) and were synthesized by Integrated DNA Technologies (IDT, Belgium) (Error! Reference source not found.). The Step One Plus real-time PCR system (Applied Biosystems, Belgium) was used for all real-time PCR assays and melt curve analyses. 20 µL reaction mixture contained 10 µL of 2 x TaqMan Universal Master Mix II (Applied Biosystems), 1 µL (10 µM) of each primer, 0.5 µL (10 µM) of probe, 2 µL template and 5.5 µL of PCR water. Each assay was run according to the conditions stated in **Table 1** in technical triplicate together with an appropriate positive control (DNA extracted from *L. donovani* promastigotes) and blank (PCR water). DNA from naïve uninfected animal tissues was included to check specificity. Resulting cT-values were converted into the number of amastigotes per gram tissue based on a 1:10 standard dilution curve of RNA extracted from infected liver or spleen samples.

Coefficients of variation of each sample were calculated by standard formulae to measure intra-assay variation.

DNA extraction and parasite quantification by DNA qPCR

Isolated spleen and liver samples were immediately preserved in 180 µL ATL buffer to allow DNA stabilization. Subsequent lysis and DNA extraction of tissue samples was performed using the QIAamp DNA Mini and Blood Mini Kit (Qiagen) according to the manufacturer's instructions. Resulting DNA concentrations and purities were estimated spectrophotometrically. Parasite burdens were determined using a quantitative Sybr Green qPCR for the *CPB* gene, a highly expressed and stable multicopy gene consisting of five copies (Hide et al. 2007). Primers ('*CPB*') amplifying an 125 bp fragment were designed and synthesized as described above (Error! Reference source not found.). 20 µL reaction mixtures contained 10 µL of 2 x Power SYBR Green PCR Master Mix (Applied Biosystems), 0.4 µL (5 µM) of each primer, 2 µL of template and 7.2 µL of PCR water. Each PCR reaction was carried out according to the conditions stated in **Table 1** in technical replicate and specificity was verified by melt curve analysis. cT-values were converted into numbers of amastigotes per gram based on a 1:10 standard dilution curve of DNA extracted from infected liver or spleen tissues as described above.

Statistical analysis

Reproducibility of the hamster model. A Kruskal-Wallis test (IBM SPSS Statistics version 22) was used to assess the reproducibility of the parasite burdens within the same experimental group (either untreated or MIL-treated) over different independent experiments. Good reproducibility would imply $p > 0.05$. Data from respectively five (*L. infantum*) and two (*L. donovani*) independent experiments with five to six animals per group were analyzed. Outliers were removed based on the built-in algorithm in SPSS.

Correlation and agreement between burdens determined by microscopy, DNA and RNA qPCR. Correlation between the obtained results with the three assays was investigated using the non-

parametric Pearson's correlation test for liver and spleen separately. In addition, the Bland-Altman plot was used to study the level of agreement between the three methods and to show dispersion of the data (Bland and Altman 1986). For this, differences between the analyzed methods were plotted against their mean. In case of comparable results, the differences should be centered around zero (one sample *t*-test, $p > 0.05$) without any proportional bias (linear regression, $p > 0.05$). All statistical analysis were performed on the original data set using SPSS.

Homogeneity of infection. Amastigote burdens derived from either microscopic counting or from DNA or RNA qPCR were calculated for each of the five pieces of the same organ. These five values were plotted against each other and expressed in percentages relative to the mean burden of the five pieces which was set at 100%. Interpretation of the variation between the different pieces of the same organ is not straightforward as each result is influenced by random variation associated with the laboratory activity (analytical variation, CVa) and by inherent biological variation (BV). The Reference Change Value (RCV) incorporates both variations and is defined as the critical difference that must be exceeded between two samples in order to be considered significant (Ozturk 2012, Ricós et al. 2009). If the variation between the burdens of pieces derived from the same organ is smaller than the RCV, the distribution of infection within that organ can be considered homogeneous. The RCV was calculated by the formula: $RCV = \sqrt{2} * Z * \sqrt{CVa^2 + BV^2} = 0.695$ or 70 % with Z = 1.96 for evaluating a bidirectional change with 95 % significance (Ozturk 2012, Ricós et al. 2009), CVa = 0.02 (the average maximal coefficient of variation in our qPCR experiments) and BV = 0.25 (Gan et al. 2007, Maes et al. 2015).

Effect of treatment on the parasite burden in the target organs. Parasite burdens in liver and spleen of untreated and MIL-treated hamsters were compared by the non-parametric Mann-Whitney U test. This analysis was independently performed on the parasite quantifications using the 3 approaches (microscopy, DNA and RNA qPCR). The difference in parasite burdens between liver and spleen samples of the same animal was assessed using the non-parametric paired Wilcoxon signed-rank test.

Results

Agreement between burdens determined by microscopy, DNA and RNA qPCR.

Parasite burdens in infected non-treated and miltefosine-treated hamsters were evaluated by conventional microscopy analysis of Giemsa-stained tissue imprints and two newly developed molecular tests based on the semi-quantitative detection of either *CPB* DNA or *18S rRNA*. PCR efficiencies for these two molecular targets were excellent for the detection of *L. donovani* and *L. infantum* in both liver and spleen as target organs (Fig S1 and S2). Both DNA and RNA qPCR show low intra-assay variation ranging from 0.08 % to 1.4 % (DNA) and 0.11 % to 3 % (RNA) with an average of 0.7 % (DNA) and 0.9 % (RNA), independent of the target tissue and *Leishmania* species. For both liver and spleen, a highly significant positive correlation ($p < 0.00001$) was found between the number of amastigotes per gram tissue determined by all three methods (**Fig 1**). In general, correlations were better in spleen than in liver tissue. DNA-based parasite detection also correlated slightly better than RNA qPCR with the liver imprints. Bland-Altman plots for both organs also showed a good agreement between all three methods with their differences centered around zero ($p > 0.05$ for the one sample *t*-test). Furthermore, no proportional bias, *e.g.* tendency for smaller or greater differences upon increasing burdens, was observed ($p > 0.05$ for the linear regression coefficient of the mean) (**Fig 2**). Related to the higher sensitivity of the qPCR, deviation from the microscopy analysis is slightly more apparent in samples with low parasite burdens.

Infection is homogenous in the major target organs

Parasite distribution determined by all three methods was homogeneous in *L. infantum* and *L. donovani* infected livers and spleens in both untreated and MIL-treated hamsters. For microscopy and DNA qPCR, over 90 % of the measurements on both organs fell within the acceptable range of 70 % variation. Samples tested by RNA qPCR showed more variation with 70 % (liver) and 90 % (spleen) of the measurements within the 70 % variation range.

Reproducibility of the hamster model and impact of MIL-treatment

The variation in amastigote burdens within the same experimental group (respectively untreated or MIL-treated) over different independent experiments was found non-significant ($p > 0.05$) for both *Leishmania* species, indicating an excellent reproducibility of the hamster infection model (**Fig 4**). MIL-treatment had a very significant ($p \leq 0.0001$) impact on parasite burdens for both species, resulting in a microscopically observed average reduction over the independent experiments of 96.0 % ± 0.6 % (liver) and 98.2 % ± 0.5 % (spleen) for *L. infantum* and 96.7 % ± 0.8 % (liver) and 98.4 % ± 0.6 % (spleen) for *L. donovani* (data are averages of reductions ± SEM observed by microscopy in the different experiments). Liver samples show significantly higher burdens than spleen samples, both before and after treatment with a stronger relative reduction in the spleen (**Fig 5**). Both DNA and RNA based molecular detection techniques show a comparable impact of MIL-treatment to microscopy that was very significant (**Fig 6**). Reduction percentages calculated using DNA qPCR results were 94.5 % (liver) and 97.6 % (spleen) for *L. infantum* and 93.3 % (liver) and 95.2 % (spleen) for *L. donovani*. RNA qPCR showed a reduction of 95.2 % and 98.9 % for *L. infantum* liver and spleen respectively, and of 96.8 % (liver) and 96.9 % (spleen) for *L. donovani*.

Discussion

Tissue amastigote burdens are generally determined by microscopic counting on Giemsa-stained organ imprints. However, this labor-intensive technique has limited sensitivity (Stauber 1958) making it less suited for evaluating low parasite burdens present after treatment or in subclinical infections. Several studies have therefore focused on qPCR as a practical alternative for *Leishmania* detection due to its high sensitivity, specificity and reproducibility (Bretagne et al. 2001, Mary et al. 2004, Tupperwar et al. 2008). Only a limited number of studies were performed in the clinically relevant hamster model and none compared the assay performance with microscopy as golden standard (Moreira et al. 2012, Srivastava et al. 2013).

Quantification by qPCR requires the use of a standard curve with a known number of parasites present in the tissue under investigation. The latter is critical as the tissue matrix can influence the qPCR efficiency and sensitivity due to the presence of inhibitors. We opted for a dilution series of heavily parasitized tissue samples that were counted by microscopy. This method is possible as counts on high parasite burdens are fairly accurate, but has the disadvantage of rendering qPCR quantifications dependent on microscopic counting. An alternative would have been to use uninfected tissue samples spiked with a promastigote dilution series, but having the minor disadvantage of using a different life cycle stage of the parasite (with a potential different gene expression pattern) and of adding parasites to the tissue instead of them being integrally part of it.

Several parasite targets have been used for qPCR, including kinetoplast DNA(kDNA) (Mary et al. 2004, Srivastava et al. 2013), genomic DNA (gDNA) (Bretagne et al. 2001, Tellevik et al. 2014) and RNA (van der Meide et al. 2008), each with their advantages and disadvantages. Although present in very high copy numbers (up to 10^4 per cell)(Brewster et al. 1998), we opted not to use kDNA since the sequence and number of kDNA copies differs between *Leishmania* species, strains and parasite stage (Mary et al. 2004, Weirather et al. 2011), making it much less suitable for absolute parasite quantification. Instead, we selected the stable multicopy *CPB* gene to enable a more accurate quantification, although its sensitivity is expected to be significantly less compared to using kDNA or RNA (Lachaud et al. 2002, van der Meide et al. 2008). When using DNA as target, detection of residual DNA of dead parasites could present a problem in drug efficacy evaluation since most anti-leishmanial compounds, including miltefosine, act progressively over time (van den Bogaart et al. 2014). Therefore and to improve sensitivity, we also included the highly expressed *18S rRNA* as target which is rapidly degraded upon parasite death (van der Meide et al. 2008). On the other hand, RNA may be less suited for quantitatively studying latent infections as quiescent organisms are transcriptionally less active or even inactive (Kloehn et al. 2015) which is particularly relevant to *Leishmania* as clinical relief after drug treatment does not necessarily imply parasitological cure (Dereure et al. 2003, Engwerda et al. 2004, Murray 2001).

For the two analyzed major target organs of VL (liver and spleen), all techniques showed a very good agreement without any proportional bias. In all cases, the correlation is stronger for spleen than for liver samples, confirming liver as a more challenging target for qPCR analysis, which is probably due to the excessive presence of bile salts and polysaccharides (OpenWetWare 2010). In combination with technical variation (induced by separate DNAse treatment, cDNA synthesis and qPCR), poor RNA stability likely accounts for the observed higher variation in the evaluation of the homogeneity of infection. As alternative, a one-step RNA qPCR with simultaneous cDNA synthesis and qPCR can be adopted as has been used by González-Andrade *et al* for the detection of *Trypanosoma* species with encouraging results (Gonzalez-Andrade et al. 2014). The present study also demonstrates for the first time homogeneous distribution of *L. infantum* and *L. donovani* infection throughout the liver and spleen in Syrian golden hamsters that were either left untreated (carrying high parasite burdens) or received MIL-treatment (carrying low parasite burdens), hereby validating the already established use of single small tissue pieces to extrapolate whole organ parasite burdens.

Following miltefosine treatment, in depth assessment of the tissue amastigote burdens using the conventional and molecular parasite detection methodologies revealed higher reduction percentages in spleen than in liver. Comparison of the DNA and RNA qPCR also reveals that no significant level of residual DNA from dead parasites was detected following treatment. The pharmacokinetic properties of miltefosine (reviewed in (Dorlo et al. 2012)) seem to be compatible with the observed higher clearance rates in the spleen. Studies in rats orally treated with unlabeled miltefosine demonstrated highest drug concentrations in the adrenal glands, kidneys, spleen and skin (Marschner et al. 1992). Recent reports also indicate that miltefosine not only exerts a direct antiparasitic activity but also elicits immune-dependent effects that could also explain the differential impact on the main target organs (Gangalum et al. 2015, Mukherjee et al. 2012).

To the best of our knowlegde, this study represents the first in-depth analysis of homogeneity of infection in the VL hamster model to validate the use of single small tissue subsamples for whole-organ quantification purposes. Two different qPCR methods targeting either gDNA or RNA that are universal

for *L. donovani* and *L. infantum* were developed as alternative to microscopic quantification. Both assays showed very good agreement and correlation to the standard microscopy technique, for both high and low level parasitemia. The observed differential impact of miltefosine treatment on the two main target organs highlights the importance of assessing tissue-level treatment outcome in preclinical evaluation of novel drug compounds.

Acknowledgements

The authors acknowledge An Matheeussen and Pim-Bart Feijens for their technical assistance. The work was funded by the Research Fund Flanders (FWO: project G051812N and scholarship 11V4315N), the Agency for Innovation by Science and Technology in Flanders (IWT: project 121474), and additionally supported by the Drugs for Neglected Diseases initiative (DNDi, Geneva, Switserland). LMPH is a partner of the 'Antwerp Drug Discovery Network' (ADDN, www.addn.be) and the Excellence Centre 'Infla-Med' (www.uantwerpen.be/infla-med).

Reference List

Bland JM, and Altman DG (1986) Statistical methods for assessing agreement between two methods of clinical measurement. Lancet 1: 307-310

Bourgeois N, Lachaud L, Reynes J, Rouanet I, Mahamat A, and Bastien P (2008) Long-term monitoring of visceral leishmaniasis in patients with AIDS: relapse risk factors, value of polymerase chain reaction, and potential impact on secondary prophylaxis. J Acquir Immune Defic Syndr 48: 13-19

Bretagne S, Durand R, Olivi M, Garin J-F, Sulahian A, Rivollet D, Vidaud M, and Deniau M (2001) Real-Time PCR as a New Tool for Quantifying *Leishmania infantum* in Liver in Infected Mice. Clinical and Diagnostic Laboratory Immunology 8: 828-831

Brewster S, Aslett M, and Barker DC (1998) Kinetoplast DNA minicircle database. Parasitol Today 14 437–438

Dereure J, Duong Thanh H, Lavabre-Bertrand T, Cartron G, Bastides F, Richard-Lenoble D, and Dedet JP (2003) Visceral leishmaniasis. Persistence of parasites in lymph nodes after clinical cure. Journal of Infection 47: 77-81

Dorlo TP, Balasegaram M, Beijnen JH, and de Vries PJ (2012) Miltefosine: a review of its pharmacology and therapeutic efficacy in the treatment of leishmaniasis. J Antimicrob Chemother 67: 2576-2597

Engwerda CR, Ato M, and Kaye PM (2004) Macrophages, pathology and parasite persistence in experimental visceral leishmaniasis. Trends Parasitol 20: 524-530

Gan CS, Chong PK, Pham TK, and Wright PC (2007) Technical, Experimental, and Biological Variations in Isobaric Tags for Relative and Absolute Quantitation (iTRAQ). Journal of Proteome Research 6: 821-827

Gangalum PR, de Castro W, Vieira LQ, Dey R, Rivas L, Singh S, Majumdar S, and Saha B (2015) Platelet-activating factor receptor contributes to antileishmanial function of miltefosine. J Immunol 194: 5961-5967

Gonzalez-Andrade P, Camara M, Ilboudo H, Bucheton B, Jamonneau V, and Deborggraeve S (2014) Diagnosis of trypanosomatid infections: targeting the spliced leader RNA. J Mol Diagn 16: 400-404

Hendrickx S, Boulet G, Mondelaers A, Dujardin JC, Rijal S, Lachaud L, Cos P, Delputte P, and Maes L (2014) Experimental selection of paromomycin and miltefosine resistance in intracellular amastigotes of *Leishmania donovani* and *L. infantum*. Parasitol Res 113: 1875-1881

Hendrickx S, Mondelaers A, Eberhardt E, Delputte P, Cos P, and Maes L (2015) In Vivo Selection of Paromomycin and Miltefosine Resistance in Leishmania donovani and L. infantum in a Syrian Hamster Model. Antimicrob Agents Chemother 59: 4714-4718

Hide M, Bras-Goncalves R, and Banuls AL (2007) Specific cpb copies within the *Leishmania donovani* complex: evolutionary interpretations and potential clinical implications in humans. Parasitology 134: 379-389

Kloehn J, Saunders EC, O'Callaghan S, Dagley MJ, and McConville MJ (2015) Characterization of metabolically quiescent *Leishmania* parasites in murine lesions using heavy water labeling. PLoS Pathog 11: e1004683

Lachaud L, Marchergui-Hammami S, Chabbert E, Dereure J, Dedet JP, and Bastien P (2002) Comparison of six PCR methods using peripheral blood for detection of canine visceral leishmaniasis. J Clin Microbiol 40: 210-215

Loria-Cervera EN, and Andrade-Narvaez FJ (2014) Animal models for the study of leishmaniasis immunology. Rev Inst Med Trop Sao Paulo 56: 1-11

Maes E, Valkenborg D, Baggerman G, Willems H, Landuyt B, Schoofs L, and Mertens I (2015) Determination of Variation Parameters as a Crucial Step in Designing TMT-Based Clinical Proteomics Experiments. PLoS ONE 10: e0120115

Marschner N, Kotting J, Eibl H, and Unger C (1992) Distribution of hexadecylphosphocholine and octadecyl-methyl-glycero-3-phosphocholine in rat tissues during steady-state treatment. Cancer Chemother Pharmacol 31: 18-22

Mary C, Faraut F, Lascombe L, and Dumon H (2004) Quantification of *Leishmania infantum* DNA by a real-time PCR assay with high sensitivity. J Clin Microbiol 42: 5249-5255

Moreira NdD, Vitoriano-Souza J, Roatt BM, Vieira PMdA, Ker HG, de Oliveira Cardoso JM, Giunchetti RC, Carneiro CM, de Lana M, and Reis AB (2012) Parasite Burden in Hamsters Infected with Two Different Strains of *Leishmania* (*Leishmania*) *infantum*: "Leishman Donovan Units" versus Real-Time PCR. PLoS One 7: e47907

Mukherjee AK, Gupta G, Adhikari A, Majumder S, Kar Mahapatra S, Bhattacharyya Majumdar S, and Majumdar S (2012) Miltefosine triggers a strong proinflammatory cytokine response during visceral leishmaniasis: role of TLR4 and TLR9. Int Immunopharmacol 12: 565-572

Mukherjee P, Ghosh AK, and Ghose AC (2003) Infection pattern and immune response in the spleen and liver of BALB/c mice intracardially infected with *Leishmania donovani* amastigotes. Immunology Letters 86: 131-138

Murray HW (2001) Tissue granuloma structure-function in experimental visceral leishmaniasis. Int J Exp Pathol 82: 249-267

OpenWetWare (2010) PCR inhibitors

Ozturk OG (2012) Using Biological Variation Data for Reference Change Values in Clinical Laboratories. Biochemistry and Analytical Biochemistry 1: e106

Purkait B, Kumar A, Nandi N, Sardar AH, Das S, Kumar S, Pandey K, Ravidas V, Kumar M, De T, Singh D, and Das P (2012) Mechanism of amphotericin B resistance in clinical isolates of *Leishmania donovani*. Antimicrob Agents Chemother 56: 1031-1041

Requena JM, Soto M, Doria MaD, and Alonso C (2000) Immune and clinical parameters associated with *Leishmania infantum* infection in the golden hamster model. Veterinary Immunology and Immunopathology 76: 269-281

Ricós C, Perich C, Minchinela J, Álvarez V, Simón M, Biosca C, Doménech M, Fernández P, Jiménez CV, Garcia-Lario JV, and Cava F (2009) Application of biological variation – a review. Biochemia Medica 19: 250-259

Srivastava A, Sweat JM, Azizan A, Vesely B, and Kyle DE (2013) Real-time PCR to quantify *Leishmania donovani* in hamsters. J Parasitol 99: 145-150

Stauber LA (1958) Host Resistance to the Khartoum Strain of *Leishmania donovani*. The Rice Institute Pamphlet 45: 80-96

Sundar S (2001) Drug resistance in Indian visceral leishmaniasis. Trop Med Int Health 6: 849-854

Tellevik MG, Muller KE, Lokken KR, and Nerland AH (2014) Detection of a broad range of *Leishmania* species and determination of parasite load of infected mouse by real-time PCR targeting the arginine permease gene AAP3. Acta Trop 137: 99-104

Tupperwar N, Vineeth V, Rath S, and Vaidya T (2008) Development of a real-time polymerase chain reaction assay for the quantification of *Leishmania* species and the monitoring of systemic distribution of the pathogen. Diagn Microbiol Infect Dis 61: 23-30

van den Bogaart E, Schoone GJ, Adams ER, and Schallig HDFH (2014) Duplex quantitative Reverse-Transcriptase PCR for simultaneous assessment of drug activity against *Leishmania* intracellular amastigotes and their host cells(). International Journal for Parasitology: Drugs and Drug Resistance 4: 14-19

van der Meide W, Guerra J, Schoone G, Farenhorst M, Coelho L, Faber W, Peekel I, and Schallig H (2008) Comparison between quantitative nucleic acid sequence-based amplification, real-time reverse transcriptase PCR, and real-time PCR for quantification of *Leishmania* parasites. J Clin Microbiol 46: 73-78

van Eys GJ, Schoone GJ, Kroon NC, and Ebeling SB (1992) Sequence analysis of small subunit ribosomal RNA genes and its use for detection and identification of *Leishmania* parasites. Mol Biochem Parasitol 51: 133-142

Weirather JL, Jeronimo SM, Gautam S, Sundar S, Kang M, Kurtz MA, Haque R, Schriefer A, Talhari S, Carvalho EM, Donelson JE, and Wilson ME (2011) Serial quantitative PCR assay for detection, species discrimination, and quantification of *Leishmania* spp. in human samples. J Clin Microbiol 49: 3892-3904

WHO (2010) Control of the leishmaniasis: report of a meeting of the WHO Expert Committe on the Control Leishmaniases. In Word Healt Organ Tech Rep Ser (Geneva: WHO), pp. 1-186

WHO (2015a) Kala-azar elimination programme. Report of a WHO consultation of partners (Geneva, Switzerland)

WHO (2015b) Leishmaniasis Fact sheet N°375, WHO, ed.

Table 1. Primer sequences and qPCR settings.

Targets	Sequence of primers and probes	Activation step	Amplification (40 cycles)	Melting curve
18S rRNA				
FP	5'-TTGGGGATCTTATGGGCCG-3'	95°C 10min	95°C 15s, 57°C 15s,	
RP	5'-GAGGATATTCCCGTGGGTGG-3'		60°C 1min	
Probe	5'-FAM-AGGGTTACCCTGTGTCAGCACCGCG-DQ-3'			
CPB				
FP	5'-AACGAAACGGTTATGGCTGC-3'	95°C 10min	95°C 15s, 60°C 1min	95°C 15s, 60°C 1min,
RP	5'-CTTGTTGTACCCGACGAGCA-3'			95°C 15s

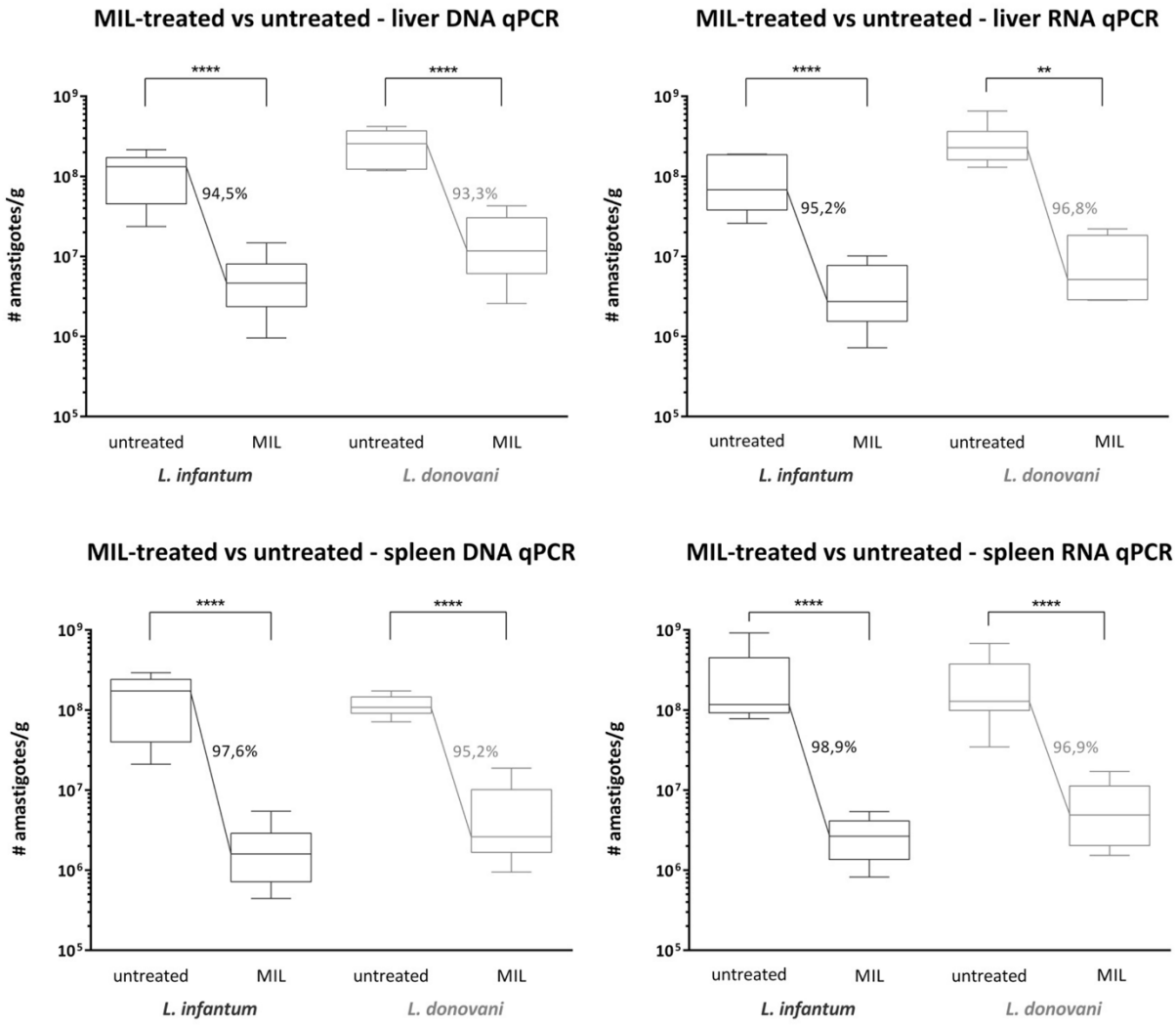

Fig 1. Comparison of conventional and molecular parasite detection methodologies. Correlations between the parasite burdens (# amastigotes/g) measured by microscopic counting of Giemsa-stained organ imprints, DNA qPCR and RNA qPCR for liver (top row) and spleen (bottom row). For each combination, the number of included data points are shown (N) as well as the Spearman's correlation coefficients (r_s). Combined data from *L. infantum* and *L. donovani* were used for the analysis.

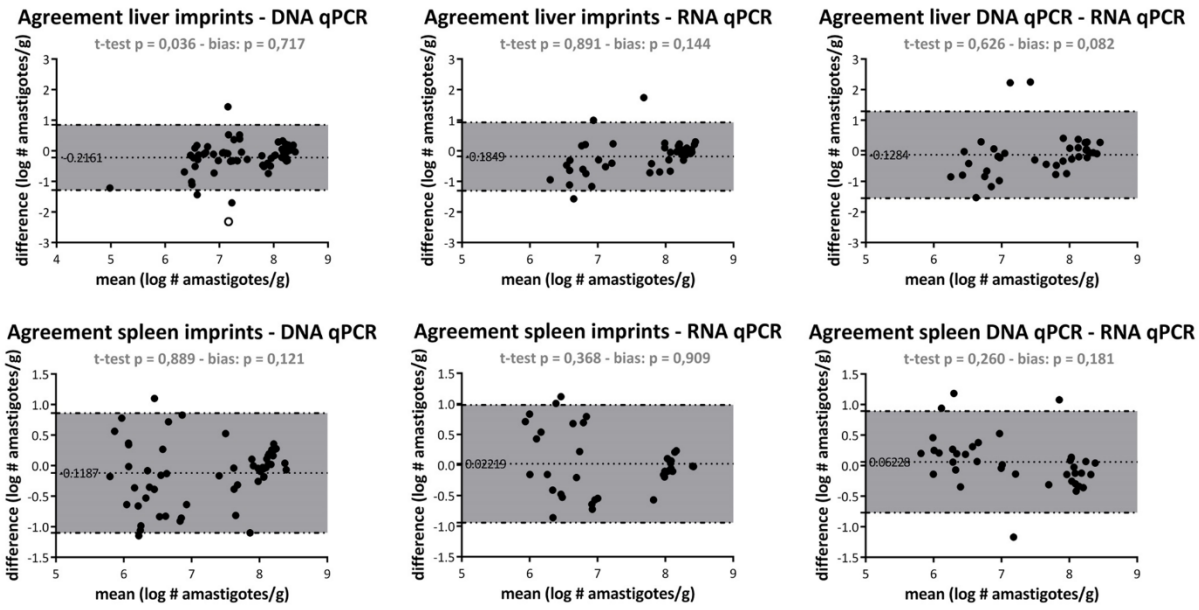

Fig 2. Variation in conventional and molecular parasite detection methodologies. Bland-Altman plots for the liver (top row) and spleen (bottom row) of the mean log parasite burdens (# amastigotes/g) determined by microscopy of Giemsa-stained organ imprints, DNA and RNA qPCR, plotted against their log burden difference. For each comparison, the mean parasite burden and estimated mean log difference are shown with indication of the 95% confidence intervals. The p-values from the one sample t-test and linear regression coefficient (bias) are also displayed. The significant difference from zero found for liver microcopy versus DNA qPCR disappeared upon removal the largest outlier (empty symbol). Combined data from *L. infantum* and *L. donovani* were used for the analysis.

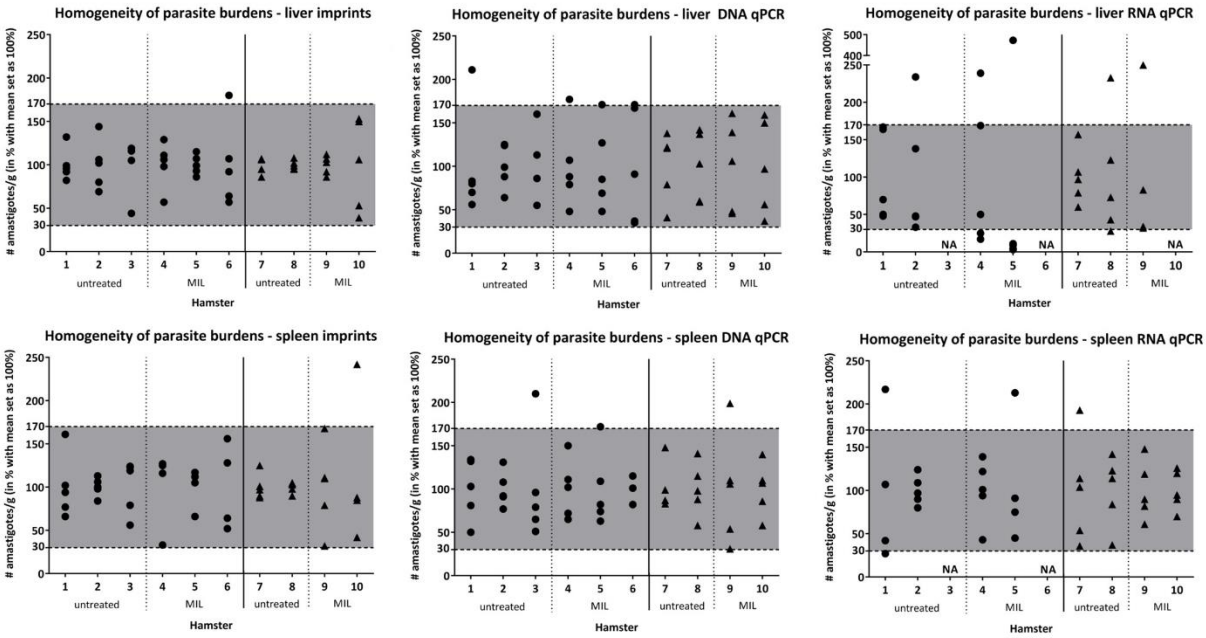

Fig 3. Homogeneity of parasite distribution in the major target organs. Parasite burdens were determined by either microscopy of Giemsa-stained imprints (left column), DNA qPCR (middle column) or RNA qPCR (right column) for livers (top row) and spleens (bottom row) originating from *L. infantum* (circles) or *L. donovani* (triangles) infected hamsters. Parasite burdens (# amastigotes/g) are expressed in percentages with the mean burden of the five pieces set as 100%. The RCV value of 70 % is indicated by the interval (30-170). NA: not available.

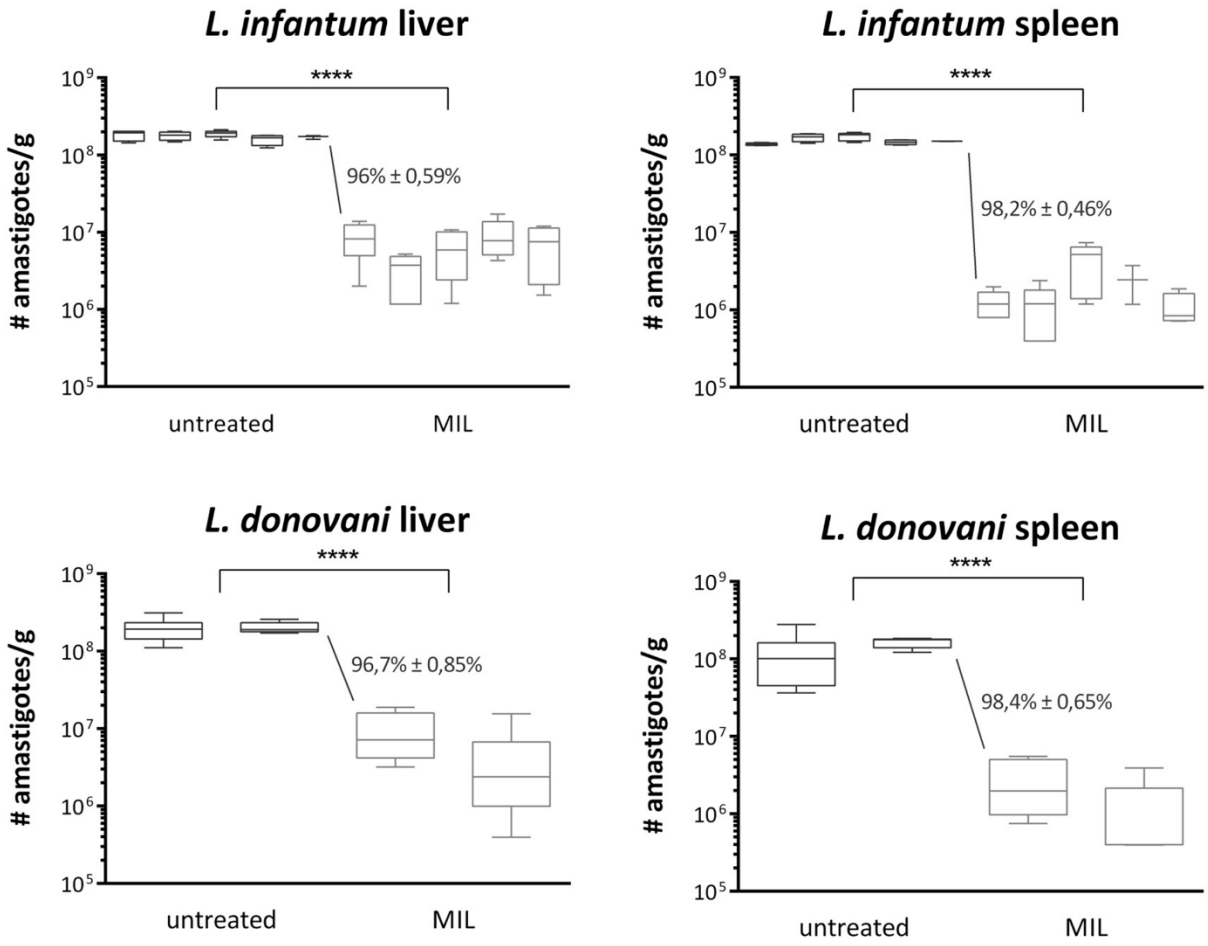

Fig 4. Reproducibility of the hamster infection model. Boxplots showing parasite burdens (# amastigotes/g) determined by microscopic counting on the same experimental group (untreated or MIL-treated hamsters) over five independent experiments for *L. infantum* (top row) and two experiments for *L. donovani* (bottom row) on both liver (left column) and spleen (right column). Each boxplot represents results from an independent infection experiment. **** indicate p-values ≤0.0001.

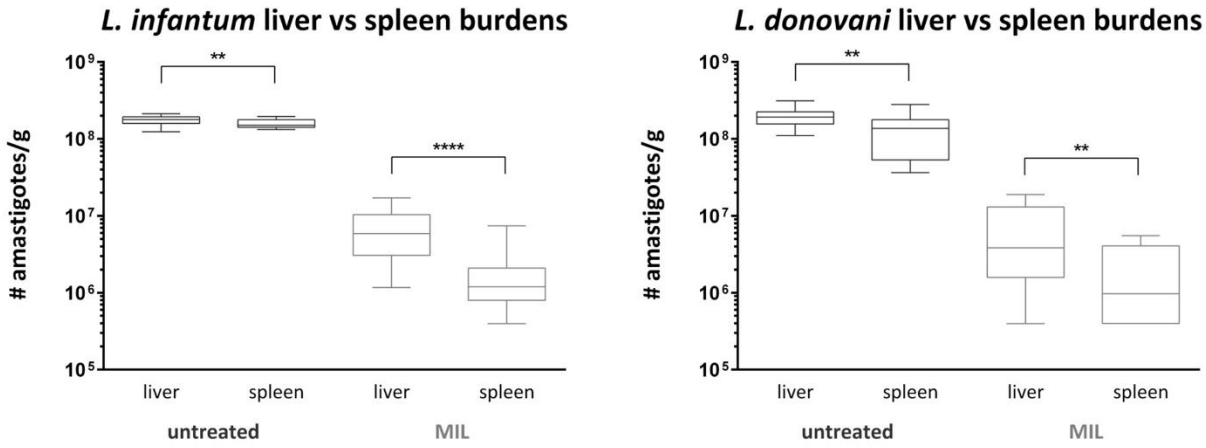

Fig 5. Comparison of parasite burdens in the main target organs. Difference in *L. infantum* (left) or *L. donovani* (right) parasite burdens (# amastigotes/g) determined by microscopic counting in liver and spleen samples of untreated (dark grey) and MIL-treated (light grey) hamsters. Parasite burdens of the independent experiments shown in Fig 4 are combined for the analysis. ** $p \leq 0.01$, **** $p \leq 0.0001$.

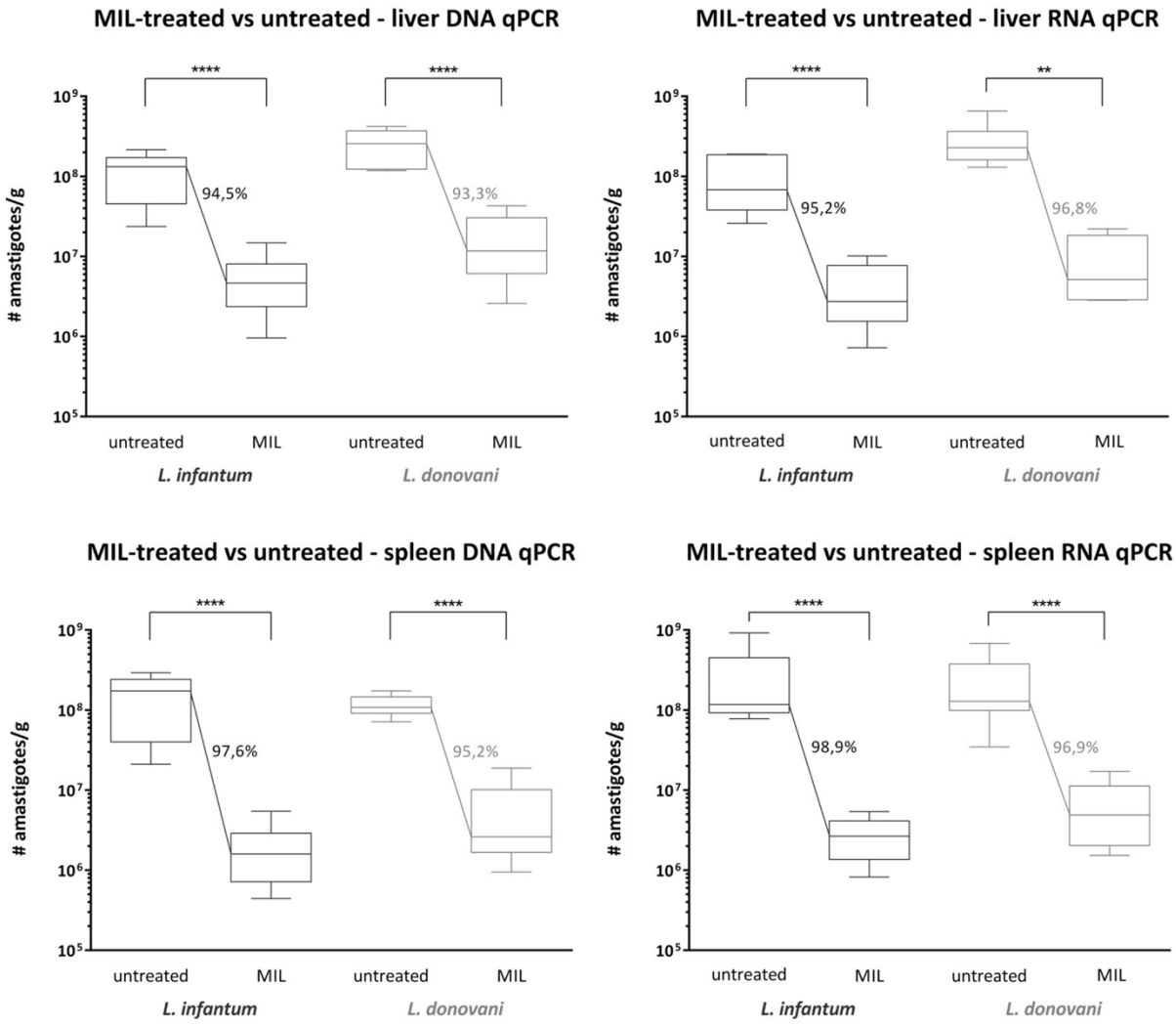

Fig 6. Impact of treatment on tissue parasite burdens. Parasite burdens (# amastigotes/g) in untreated and MIL-treated hamsters determined by either DNA qPCR (left column) or RNA qPCR (right column) on livers (top row) and spleens (bottom row) originating from *L. infantum* (dark grey) or *L. donovani* (light grey) infected hamsters. Amastigote burdens of all five pieces of the same organ are plotted together for each treatment group and parasite species. **p ≤0.01, ****p ≤0.0001

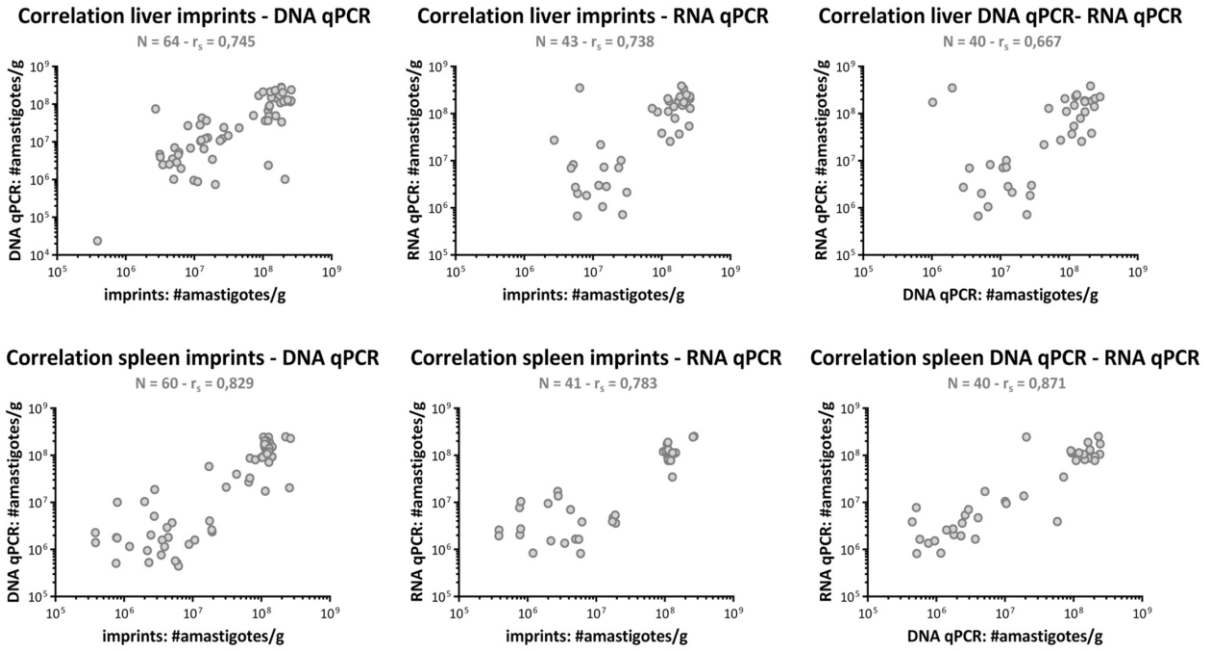

Fig S1. Linearity and PCR efficiency for *L. infantum*. Standard curves of the CPB DNA qPCR (top row) and 18S rRNA qPCR assay (bottom row) for liver (left) and spleen (right) with standard deviations on each data point.

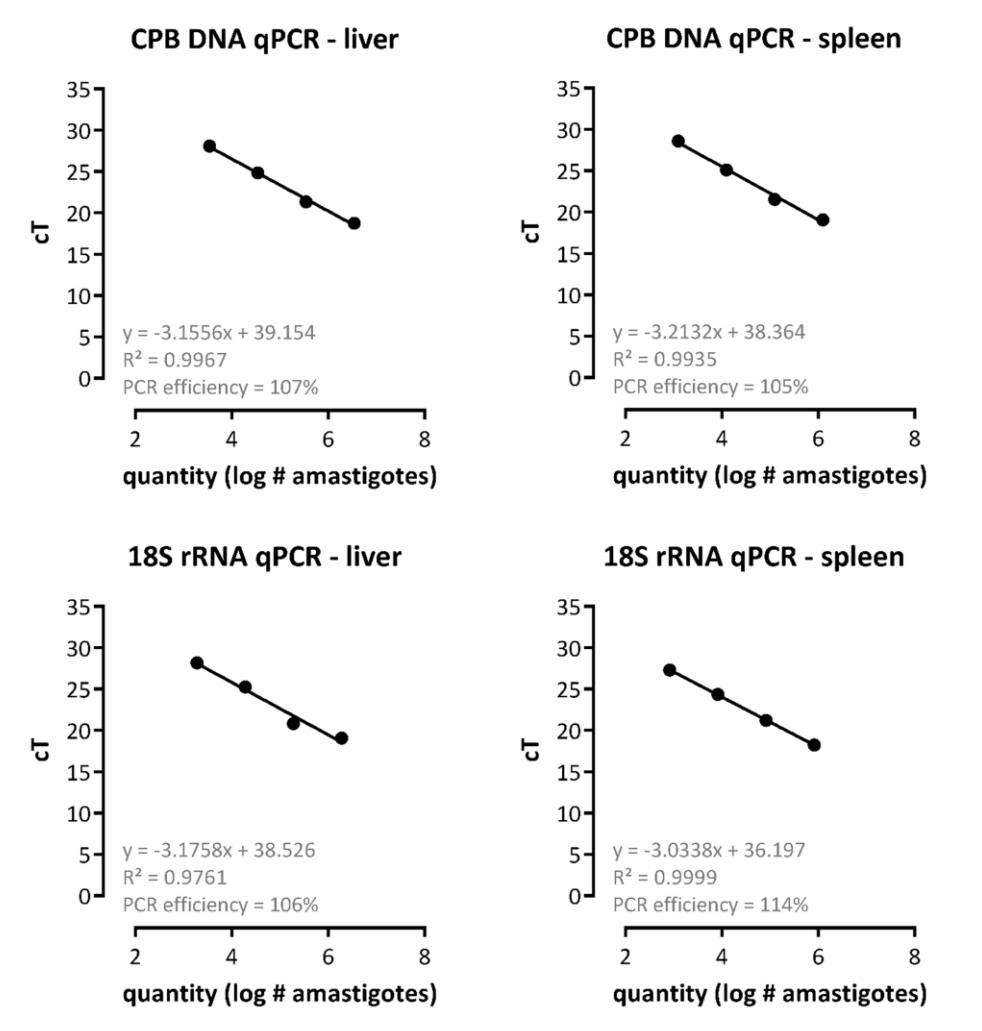

Fig S2. Linearity and PCR efficiency for *L. donovani*. Standard curves of the CPB DNA qPCR (top row) and 18S rRNA qPCR assay (bottom row) for liver (left) and spleen (right) with standard deviations on each data point.